Development 133, 4109-4118 (2006) doi:10.1242/dev.02563

Shroom2 (APXL) regulates melanosome biogenesis and localization in the retinal pigment epithelium

Pamela D. Fairbank[1], Chanjae Lee[1], Avegiyel Ellis[1,*], Jeffrey D. Hildebrand[2], Jeffrey M. Gross[1,3] and John B. Wallingford[1,3,†]

Shroom family proteins have been implicated in the control of the actin cytoskeleton, but so far only a single family member has been studied in the context of developing embryos. Here, we show that the Shroom-family protein, Shroom2 (previously known as APXL) is both necessary and sufficient to govern the localization of pigment granules at the apical surface of epithelial cells. In *Xenopus* embryos that lack Shroom2 function, we observed defects in pigmentation of the eye that stem from failure of melanosomes to mature and to associate with the apical cell surface. Ectopic expression of Shroom2 in naïve epithelial cells facilitates apical pigment accumulation, and this activity specifically requires the Rab27a GTPase. Most interestingly, we find that Shroom2, like Shroom3 (previously called Shroom), is sufficient to induce a dramatic apical accumulation of the microtubule-nucleating protein γ-tubulin at the apical surfaces of naïve epithelial cells. Together, our data identify Shroom2 as a central regulator of RPE pigmentation, and suggest that, despite their diverse biological roles, Shroom family proteins share a common activity. Finally, because the locus encoding human SHROOM2 lies within the critical region for two distinct forms of ocular albinism, it is possible that *SHROOM2* mutations may be a contributing factor in these human visual system disorders.

KEY WORDS: Shroom, Shroom2, Retina, RPE, APXL, Melanosome, Ocular albinism

INTRODUCTION

The retinal pigment epithelium (RPE) is a single-cell thick epithelium located at the posterior of the eye, apposed between the neural retina and the choroidal vasculature. One of the crucial physiological functions of the RPE is to absorb stray light that has not interacted with retinal photoreceptors, light that if otherwise unimpeded would result in backscatter and a loss of visual acuity (Back et al., 1965). RPE pigmentation is a result of the accumulation of melanosomes-modified lysosomes that contain a dense array of black pigment granules. Melanosome biogenesis and localization in the RPE requires several identified proteins including tyrosinase, AP3, members of the BLOC complex, Rab27a and OA1. Many of the genes encoding these proteins are mutated in human genetic disorders that affect RPE pigmentation, underscoring their importance in the process (for reviews, see Marks and Seabra, 2001; Raposo and Marks, 2002).

The biogenesis of melanosomes from endosomes is a multistep process involving a suite of protein components (Marks and Seabra, 2001; Raposo and Marks, 2002). Once formed, mature melanosomes are deployed to the apical surface of the RPE via both microtubule and actin cytoskeletons (Barral and Seabra, 2004). Melanosomes first move to the apical surface along microtubule tracks and are then thought to be transferred to an apical actin network through which they are deployed to their final positions (Burnside et al., 1983; Gibbs et al., 2004; King-Smith et al., 1997; Maniak, 2003; McNeil et al., 2004; Troutt and Burnside, 1989). Indeed, molecules involved in melanosome deployment also underlie some human visual system disorders. For example, mutations in Rab27a result in Griscelli syndrome Type I, a disorder in which the movement of melanosomes along actin filaments is disrupted (Seabra and Coudrier, 2004). Although microtubules are known to be essential for the maturation and positioning of endosomes (Apodaca, 2001; Bomsel et al., 1990), no microtubule regulators have yet been identified as essential for melanosome positioning or biogenesis.

In this paper, we report that Shroom2 (previously called APXL) (Schiaffino et al., 1995b) is essential for the proper pigmentation of the RPE. Shroom family proteins are marked by regions of significant protein sequence similarity between different family members (Fig. 1A); however, to date, each member has been found to govern apparently unrelated biological processes (Hagens et al., 2006). The most thoroughly studied family member, Shroom3, encodes an actin-binding protein that is essential for apical constriction, a cell shape change that is crucial to vertebrate neural tube closure (Haigo et al., 2003; Hildebrand, 2005; Hildebrand and Soriano, 1999). Shroom1 (previously called APX) is thought to link Na^+ channel activity to the actin cytoskeleton (Prat et al., 1996; Staub et al., 1992; Zuckerman et al., 1999), whereas a third member of the family, Shroom4 (previously called KIAA1202), has recently been shown to be mutated in humans with X-linked mental retardation (Hagens et al., 2005). Recent studies have implicated Shroom2 in regulating the actin cytoskeleton (Dietz et al., 2006), but no in vivo developmental studies of Shroom2 have yet been reported.

In *Xenopus* embryos lacking Shroom2 function, we find that defects in RPE pigmentation stem from failures of melanosomes to mature and to associate with the apical cell surface. Ectopic expression of Shroom2 in naïve epithelial cells facilitates apical pigment accumulation, and this activity specifically requires the Rab27a GTPase. Most interestingly, we find that Shroom2 shares at least one cellular activity with Shroom3: either protein is sufficient to induce a dramatic apical accumulation of the microtubule-nucleating protein γ-tubulin in naïve cells. Together, our data identify Shroom2 as a central regulator of RPE pigmentation, and suggest that, despite their diverse biological roles, Shroom family proteins share at least one common cellular activity.

[1]Section of Molecular Cell and Developmental Biology, Institute for Cellular and Molecular Biology, University of Texas, Austin, TX 78712, USA. [2]Department of Biological Sciences, University of Pittsburgh, Pittsburgh, PA 15260, USA. [3]Institute for Neuroscience, University of Texas, Austin, TX 78712, USA.

*Present address: University of North Texas Health Science Center, Texas College of Osteopathic Medicine, Fort Worth, TX 76107, USA
†Author for correspondence (e-mail: wallingford@mail.utexas.edu)

Accepted 3 August 2006

MATERIALS AND METHODS

Embryo assays

For blastula assays (Figs 1, 2), one blastomere of a four-cell embryo was injected animally. Embryos were then cultured to stage 8. For morpholino assays (Figs 5-7), two left blastomeres or all four blastomeres of a four-cell embryo were injected animally. Embryos were then cultured to various tadpole stages (27-42). Standard methods were used throughout (Sive et al., 2000), and embryos were staged according to Nieuwkoop and Faber (Nieuwkoop and Faber, 1994). Embryos were imaged using a Leica MZ16FA stereoscope and subsequently processed in Adobe Photoshop 7.0.

In situ hybridization

Whole-mount in situ hybridization was carried out on *Xenopus* embryos as described previously (Sive et al., 2000). Whole-mount embryos were then imaged using a Leica MZ16FA stereoscope. Subsequently, embryos were prepared for cryosectioning by fixing in MEMFA overnight at 4°C, washing three times for five minutes in PBS + 0.1% Tween-20, then cryoprotecting by immersion in 25% sucrose at room temperature until equilibrated and increased to 40% sucrose overnight at 4°C. Embryos were frozen in TBS tissue freezing medium (Triangle Biomedical Sciences), sectioned at 12 μm in a cryostat and collected on gelatin-coated slides. Slides were then mounted either temporarily with 90% glycerol + 10% 1× PBS, or permanently with DPX (Electron Microscopy Sciences) and imaged using a Zeiss Axioplan 2 mounted with SPOT digital camera. Images were subsequently processed using Adobe Photoshop 7.0.

Morphometrics

For cell-surface area measurements, mRNA was injected animally into one blastomere of a four-cell embryo. Embryos were then cultured until stage 8. Embryos were then fixed in MEMFA overnight at 4°C, then rinsed three times for five minutes in PBS + 0.1% Tween-20. Embryos were then imaged using a Leica MZ16FA stereoscope. Cells were individually traced and surface area calculated using Image-Pro Plus software. For morphant eye pigmentation comparison, embryos were injected as described, cultured, fixed, washed and imaged using a Leica MZ16FA stereoscope. Eyes were then individually traced and pixel density calculated for each in Image-Pro Plus. For melanosome morphometrics, TEM images were loaded into Image-Pro Plus software and analyzed using the roundness and area functions.

Actin visualization

Embryos were fixed overnight at 4°C in MEMFA, then rinsed three times for five minutes in PBS + 0.1% Tween-20. Embryos were then incubated in 4 U/ml of Oregon Green 488 phalloidin (Molecular Probes) in PBS + 0.1% Tween-20 overnight at 4°C. Just before visualization on a Zeiss LSM5 PASCAL confocal microscope, embryos were rinsed twice for 10 minutes in PBS + 0.1% Tween-20. Images were subsequently processed using Adobe Photoshop 7.0.

Cloning of Shroom2(576-882), truncShroom2 and design of morpholino oligonucleotides

A dominant-negative fragment of mouse Shroom2 was amplified from CS3+MT-mouse Shroom2 by PCR using Turbo Pfu polymerase (Stratagene) and the following primer set: 5′-ACTATGGCCAGCCG-CACTGTGAGAAC-3′ and 5′-CAGTGACCTCTTCTGGAACC-3′ (spanning amino acids 576-882). After addition of 3′A-overhangs post-amplification by Taq polymerase, the PCR product was cloned into TOPO vector (Invitrogen) and then transferred into CS2+.

A truncated version of Shroom2, similar to the Shroom2-SPL-MO splice product, was created from CS3+MT-mouse Shroom2 by cutting with *Sac*I inside the ASD2 domain, followed by *Sal*I, blunting with Klenow, cutting the 5′ end with *Bam*HI, and ligating into CS107-3STOP at the *Eco*RV site. Blastula assays were performed as described above.

For morpholino oligonucleotide design, genomic sequence for Shroom2 was obtained by BLAST search of trace files from the Joint Genome Institute *Xenopus tropicalis* genome project. Equivalent regions of *X. laevis* Shroom2 were amplified by PCR with primers designed against the *X. tropicalis* sequence. The *X. laevis* genome sequence was used to design an MO against the 5′ splice acceptor site between the ASD1 and ASD2 domains of Shroom2. The sequence of the Shroom2-SPL-MO is 5′-TAC-TACCATACACACCTTGACAAGT-3′. RT-PCR to check the splicing product was performed with the following primers: Shroom2-spl-up 5′-TGGAATGGAACCGTCTG-3′ and Shroom2-spl-dn 5′-GTGTCT-GCTTTCCTTCTCAG-3′. The sequence of the control mismatch morpholino (Shroom2-5MM-MO), which was derived from Shroom2-SPL-MO and mismatched at five positions (lowercase), is 5′-TAgTACgATACAgACCTTcACAAcT-3′.

The GenBank Accession Number for Shroom2 in *Xenopus tropicalis* is: DQ886532.

Lipofection

CS2+mouse Shroom2(576-882) DNA plasmid was transfected into the eye field of stage 18 embryos using a technique described previously (Ohnuma et al., 2002). CS2+memEGFP plasmid DNA was co-transfected to mark the transfected cells. All plasmids were mixed with DOTAP (Roche) at a ratio of 1 μg of plasmid DNA to 3 μl of DOTAP. Embryos were cultured to stage 42 and fixed overnight at 4°C in MEMFA, then rinsed three times for five minutes in PBS + 0.1% Tween-20 and imaged using a Leica MZ16FA fluorescence stereoscope. Images were subsequently processed using Adobe Photoshop 7.0.

Histology and transmission electron microscopy

Embryos were fixed overnight at 4°C in 1% (w/v) paraformaldehyde, 2.5% glutaraldehyde, 3% sucrose in PBS. They were then briefly washed three times in PBS and post-fixed in 1% OsO_4 for 1 hour at 4°C, after which they were again briefly washed three times in PBS and dehydrated through a graded ethanol series (50%, 70%, 80%, 90% and 2 × 100%). Embryos were further dehydrated twice for 10 minutes in propylene oxide and infiltrated for 1-2 hours in a 50% propylene oxide/50% Epon/Araldite mixture (Polysciences). They were then incubated overnight in 100% Epon/Araldite resin in Eppendorf tubes with caps opened to allow for propylene oxide evaporation and resin infiltration. Embryos were embedded into plastic molds and baked at 60°C for 2 days. Histological sections 1 μm thick were cut, heat mounted on glass slides, stained with a 1% Methylene Blue/1% borax solution and imaged on a Leica DMLB mounted with a Leica DFC320 digital camera. For transmission electron microscopy, transverse sections were cut through the central retina, 60-80 nm in thickness, and mounted onto slot grids. Sections were stained with lead citrate and uranyl acetate. Images were obtained on a Philips EM 208 transmission electron microscope (80 kV) via an AMT Advantage HR 1MB digital camera. Images were subsequently processed using Adobe Photoshop CS.

Antibody staining

Fixed embryos were dehydrated completely in methanol and were bleached in 10% hydrogen peroxide/67% methanol for 3 hours and rehydrated consecutively with TBS (155 mM NaCl, 10 mM Tris-Cl, pH 7.4). To reduce autofluorescence of yolk platelets, the embryos were incubated with 100 mM $NaBH_4$ in TBS for 4 hours at room temperature or overnight at 4°C and rinsed in TBST (0.1% Triton X-100 in TBS). γ-Tubulin or myc-tagged mouse Shroom2 was detected by rabbit polyclonal anti-γ-tubulin (1:200 dilution) or monoclonal anti-myc (1:1000 dilution, Sigma) antibody diluted in FBS solution (TBS containing 10% fetal bovine serum and 5% DMSO). Primary antibodies were detected with Alexa Fluor 488 goat anti-rabbit IgG (Molecular Probes), or Alexa-555 goat anti-mouse IgG (Molecular Probes) diluted 1:250 in FBS solution. Embryos were cleared in Murray's Clear solution (benzyl benzoate:benzyl alcohol=2:1).

RESULTS

Shroom2 induces pigment accumulation in naïve epithelial cells

Shroom2 has three regions of protein sequence similarity with Shroom3: an N-terminal PDZ domain and a central ASD1 (APX/Shroom Domain) and a C-terminal ASD2 domain (Fig. 1A). Shroom3 has previously been shown to regulate apical constriction in vivo during *Xenopus* and mouse neurulation (Haigo et al., 2003; Hildebrand and Soriano, 1999). In these studies, ectopic expression of Shroom3 in naïve cells resulted in pigment accumulation, apical

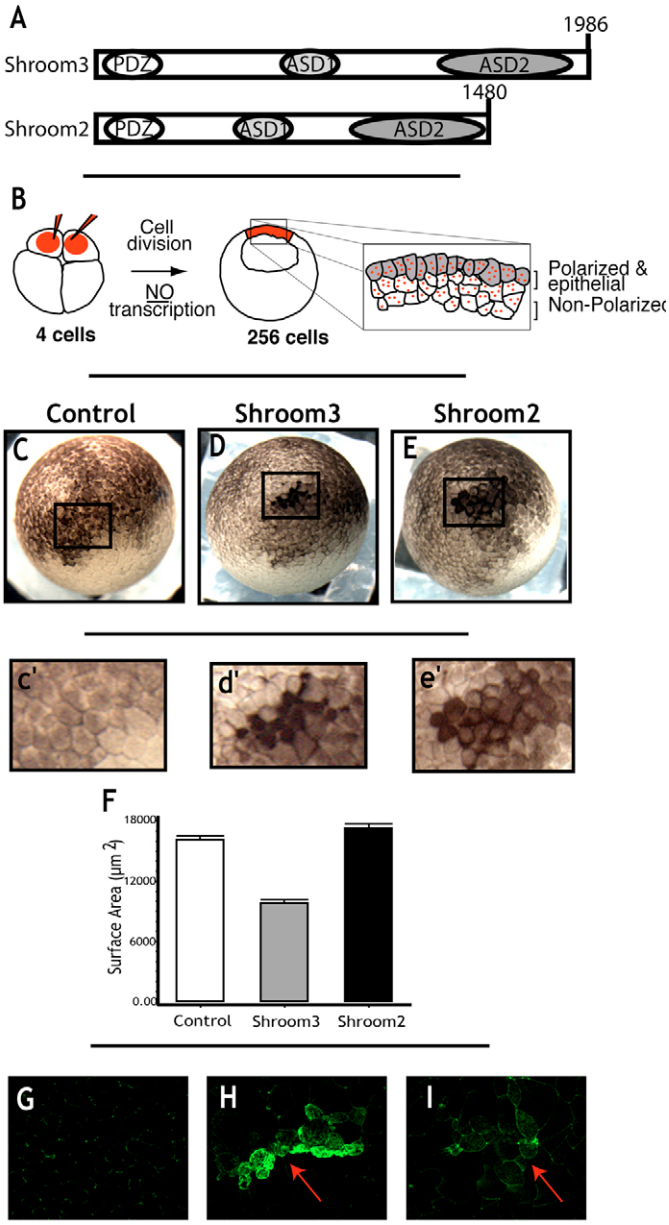

Fig. 1. Shroom2 induces apical pigment accumulation but not apical constriction in epithelial cells. (**A**) Shroom2 shares three regions of protein similarity with Shroom3, an N-terminal PDZ domain and two ASD domains. (**B**) The blastula assay. *Xenopus* blastomeres at the cleavage stages undergo cell division without transcription (Newport and Kirschner, 1982), and through asymmetric divisions, give rise to both outer, polarized epithelial cells and inner, non-polarized cells (Chalmers et al., 2003). mRNA (red) injected in individual blastomeres at the four-cell stage is distributed to polarized (grey) and non-polarized (white) cells. (**C**,**c'**) Control *Xenopus* embryos with normal levels of apical pigment. (**D**,**d'**) Embryos injected at the four-cell with 1 ng of Shroom3 or Shroom2. (**E**,**e'**) Dramatic apical pigment accumulation. (**F**) Shroom3 expression results in apical constriction and a reduction of surface area, while Shroom2 expression had no effect on cell surface area. (**G-I**) Actin localization is limited to cell junctions in control (G) cells, while Shroom3-injected embryos (H) had high levels of ectopic actin accumulation at their apical surfaces. Shroom3-injected cells accumulate only modest amounts of apical actin (I). Actin accumulation is indicated by red arrows.

constriction, and actin accumulation at the apical cell surface (Haigo et al., 2003). Given that the role of Shroom2 during development is currently unknown, and given its significant protein similarity to Shroom3, we hypothesized that it might function similarly.

During the cleavage stages in *Xenopus*, the superficial blastomeres provide a naïve epithelial cell population that is not yet transcriptionally active (Fig. 1B) (Chalmers et al., 2005; Roberts et al., 1992). Thus, when mRNA is ectopically expressed in these cells, phenotypic defects can be attributed to direct effects of the exogenous protein. This cell population has proven to be useful for studying the effects of misexpressed proteins on epithelial cell behavior (Chalmers et al., 2005; Dollar et al., 2005; Haigo et al., 2003).

When compared with uninjected control cells, expression of ectopic Shroom2 in naïve blastomeres induced a dramatic accumulation of pigment, similar to that elicited by ectopic Shroom3 (Fig. 1C-E). Interestingly, although expression of Shroom3 resulted in a significant constriction of apical cell surface area, expression of Shroom2 did not (Fig. 1D,d′,E,e′,F). Moreover, whereas apical constriction of Shroom3-expressing cells is associated with robust accumulation of actin at the apical cell surface (Fig. 1G,H) (see also Haigo et al., 2003), the accumulation of pigment in Shroom2-expressing cells was not (Fig. 1I).

Combined, these observations indicate that although Shroom2 is capable of mediating pigment redistribution in epithelial cells, its mechanism of action differs from Shroom3. Shroom2 does not induce apical actin accumulation or apical constriction. That Shroom2 does not possess these abilities seems to suggest that not all Shroom family proteins function in a similar manner.

Expression of dominant-negative Shroom2 disrupts pigmentation of the RPE

In studies of Shroom3 function, a fragment containing the ASD1 domain (spanning amino acids 754-1108) was shown to act as a dominant-negative; expression of Shroom3(754-1108) inhibited Shroom3-induced pigment accumulation and apical actin accumulation in a dose-dependent manner (Haigo et al., 2003). We asked if a similar fragment of Shroom2 would likewise behave in a dominant-negative manner. The corresponding fragment of Shroom2 spans amino acids 576-882, and indeed, co-expression of Shroom2(576-882) in naïve blastomeres blocked the activity of ectopic Shroom2 in a dose-dependent manner (Fig. 2A-D). This observation indicates that the ASD1 domain of Shroom2 does behave as a dominant-negative, and suggests that this domain might link the melanosome related functions of both Shroom3 and Shroom2.

Shroom2 is expressed strongly in the eye of humans (Schiaffino et al., 1995b), mice (Dietz et al., 2006) and *Xenopus* (Fig. 3). At the early stages of eye development, Shroom2 mRNA is expressed throughout the eye field, and with maturation of the eye Shroom2 mRNA expression becomes specific to the RPE (Fig. 3A,B). Additionally there is Shroom2 mRNA expression in the brain, ear, somites and kidney (Fig. 3A,a′ and data not shown).

Because ectopic Shroom2 induces pigment accumulation in naïve cells (Fig. 1) and endogenous Shroom2 is expressed in the RPE, we hypothesized that Shroom2 may function in regulating pigmentation. To test this hypothesis, we took advantage of the dominant-negative activity of Shroom2(576-882), and to express the construct specifically in the eye, we employed a lipofection technique developed for this purpose (Fig. 4A) (Ohnuma et al., 2002). Liposomes containing plasmid DNA were injected into the eye field at stage 18, when embryos are in the early stages of eye evagination, and lipofected embryos were allowed to develop to tadpole stages (stage 42).

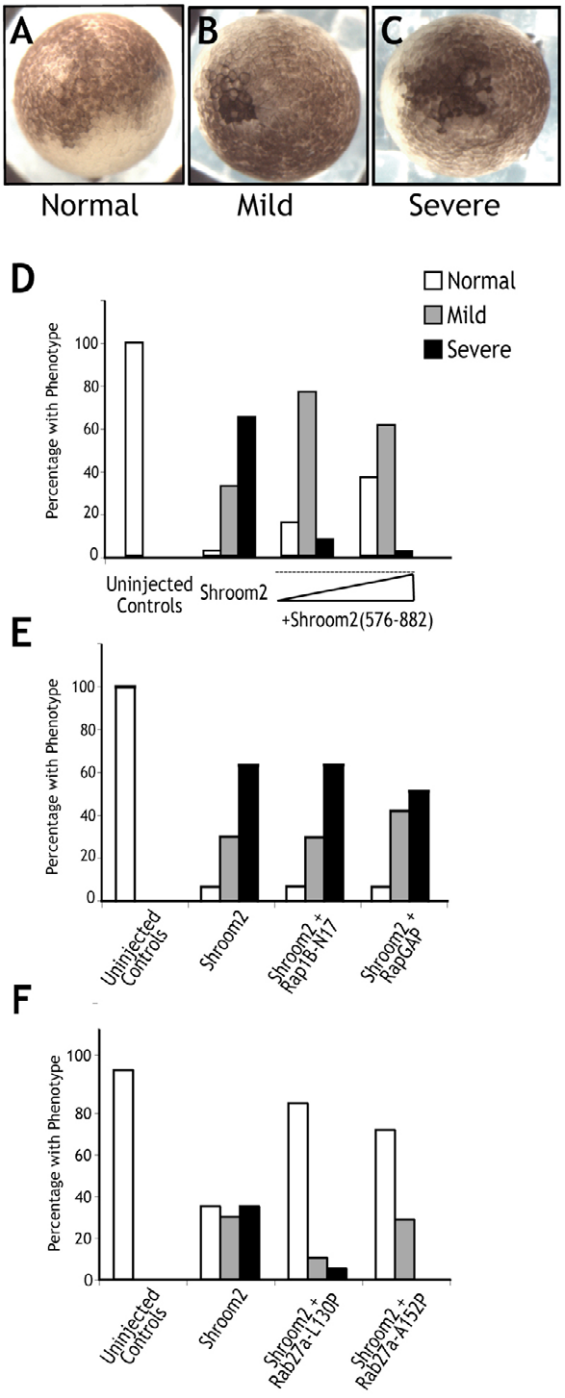

Fig. 2. Assays of Shroom2 activity. (**A-C**) Shroom2 activity was measured by blind-scoring of pigment accumulation in injected embryos. Panels A-C show representative embryos displaying normal, mild and severe phenotypes for the scoring shown in D-F. (**D**) Shroom2 (576-882) blocked the ability of ectopic Shroom2 to induce apical pigment accumulation in a dose-dependent manner. Shroom2 (0.4 ng) was injected alone or in combination with 0.8 ng or 1.6 ng of Shroom2(576-882) in one blastomeres at the four-cell stage. (**E**) Shroom2 does not function through the Rap1B GTPase. Shroom2 (0.75 ng) was injected alone or in combination with 2 ng of Rap1B-N17 or RapGAP into one blastomere at the four-cell stage. (**F**) Shroom2 acts upstream of Rab27a as co-expression of either dominant-negative Rab27a-L130P or Rab27a-A152P inhibited Shroom2 activity. Shroom2 (0.4 ng) was injected alone or in combination with 1.2 ng of Rab27a-L130P or Rab27a-A152P into one blastomere at the four-cell stage.

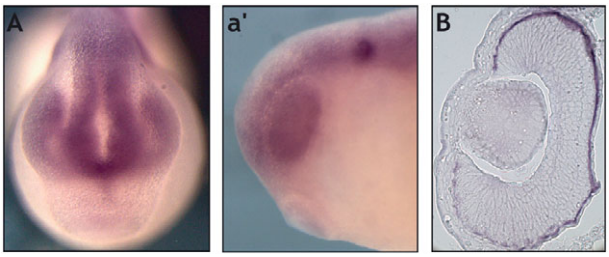

Fig. 3. Shroom2 is expressed in the eye. (**A**,**B**) In situ hybridization reveals Shroom2 mRNA is expressed in the developing eye. (A,a′) Shroom2 is expressed in the early eye field of stage 25 embryos, as well as the brain and ear. (B) Stage 40 embryos have Shroom2 mRNA expression restricted to the RPE.

Expression of Shroom2(576-882) by lipofection resulted in a dramatic disruption of eye pigmentation (Fig. 4C). In addition to this patchy hypopigmentation, eyes with Shroom2(576-882)-expressing lens cells appeared to have an abnormal lens (Fig. 4B,C). Previous experiments demonstrate that co-lipofected plasmids are almost uniformly co-expressed (Ohnuma et al., 2002), so we lineage-traced our lipofections with co-lipofected GFP. In all cases, hypopigmented regions of Shroom2(576-882)-expressing eyes displayed high levels of GFP fluorescence (Fig. 4c′). Using the same method, expression of GFP alone had no effect on eye morphology or pigmentation (Fig. 4B,b′).

Morpholino-mediated knockdown of Shroom2 disrupts pigmentation of the RPE

To confirm our findings concerning Shroom2 function, a morpholino antisense oligonucleotide (Shroom2-SPL-MO) was designed against a Shroom2 splice acceptor site between the ASD1 and ASD2 domains. Injection of this MO should disrupt normal Shroom2 splicing and results in translation of a truncated Shroom2 protein lacking the C-terminal ASD2 domain. A Shroom2 deletion construct similar to the protein predicted to be expressed in Shroom2-SPL-MO-injected embryos was designed, and gain-of-function assays confirmed that the truncated Shroom2 protein was nonfunctional (not shown). RT-PCR of injected embryos confirmed the ability of the morpholino to disrupt splicing, as normally-spliced Shroom2 mRNA was absent from Shroom2-SPL-MO injected ‘morphants’ (Fig. 5A).

Injection of Shroom2-SPL-MO into two animal blastomeres at the four-cell stage (Fig. 5B) resulted in severe defects in RPE pigmentation when assayed at stages 35 and 39 (Fig. 5C-e′) and compared with stage-matched controls. From our Shroom2-SPL-MO sequence, we designed a mismatch control morpholino with five mismatched base pairs (Shroom2-5MM-MO). This MO is unable to bind to the target site of our Shroom2-SPL-MO and therefore cannot disrupt splicing. Our Shroom2-5MM-MO control morphants had no defects in pigmentation (Fig. 5D,d′,F) indicating that our Shroom2-SPL-MO knockdown phenotype is specific and not an artifact of morpholino toxicity. Our findings that either mosaic dominant-negative Shroom2(576-882) expression or Shroom2 morpholino knock-down results in significant defects in RPE pigmentation and indicate that Shroom2 functions at some level in the regulation of this process.

Proper RPE development is known to be necessary for several aspects of vertebrate eye development and most notably for retinal lamination (e.g. Raymond and Jackson, 1995; Jensen et al., 2001). Given the striking RPE hypopigmentation in both dominant-negative Shroom2(576-882) mosaic embryos and in Shroom2-SPL-MO

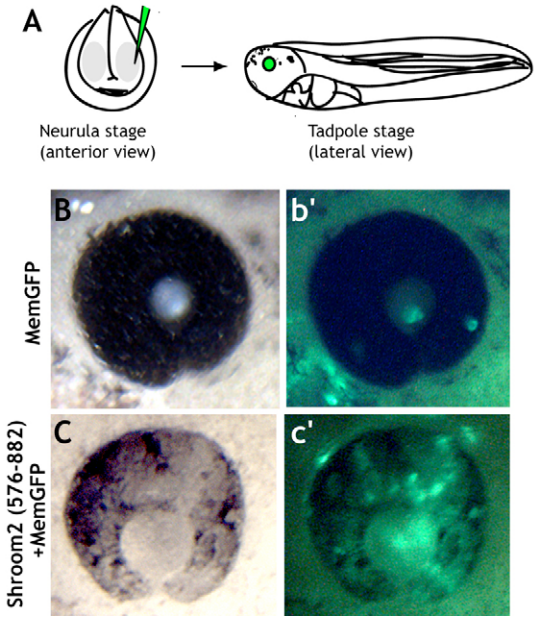

Fig. 4. Mosaic expression of a dominant-negative fragment of Shroom2 disrupts eye pigmentation. (**A**) Lipofection enables mosaic expression of dominant-negative Shroom2 specifically in the *Xenopus* eye. Constructs are lipofected into the eye field at stage 18 and grown to stage 42. All constructs are mixed at a ratio of 1 μg plasmid/3 μl DOTAP and pulsed in 10 nl volumes. (**B**,b′) Lipofection of membrane GFP alone results in normal eye morphology and pigmentation (melanin in the RPE obscures GFP fluorescence in b′). (**C**,c′) Embryos lipofected with membrane GFP and Shroom2(576-882) showed patchy hypopigmentation in areas where GFP was localized.

morphants, we assessed overall eye development in the absence of Shroom2 function. Shroom2-SPL-MO morphant eyes were often smaller in size but contained all ocular structures. In severely affected Shroom2-SPL-MO morphant eyes the lens was smaller and malformed, and the cornea appeared thicker; additionally, cell shapes in these tissues were sometimes abnormal (Fig. 6A,D; data not shown). When viewed histologically, the most severely affected Shroom2-SPL-MO morphants often showed prominent retinal lamination defects when compared with stage-matched controls and Shroom2-SPL-MO morphants showed increased numbers of pyknotic nuclei in their retinas (Fig. 6A,D). Less severely affected Shroom2-SPL-MO morphant retinas displayed significantly better retinal lamination, although pigmentation defects were still obvious (Fig. 6B,E).

Even in mildly affected morphants, we observed that in addition to pigmentation defects, the overall morphology of the RPE was defective. Phalloidin staining demonstrated that in control embryos the RPE had a very regular appearance with apical cell membranes arranged in a linear fashion (Fig. 6B,b′,C). In Shroom2-SPL-MO morphants, this regular arrangement was disturbed and membrane protrusions were often observed invading the adjacent neural retina (Fig. 6E,e′,F). Transmission electron microscopy (TEM) analysis highlights these protrusions and the irregularity of cell shapes in the RPE of Shroom2-SPL-MO morphants (Fig. 6C,F).

Melanosome localization and biogenesis is defective in Shroom2 morphants

TEM analysis also demonstrated that although melanosomes were clearly present in Shroom2-SPL-MO morphants, their distribution was not limited to the apical surface, as is the case in control RPE (Fig. 6C,F). This failure of melanosome positioning is suggestive of a defect in some aspect of RPE polarization. Such a failure of RPE polarization could explain the retinal lamination defects observed in Shroom2-SPL-MO morphants (Fig. 6), as defective polarization of the RPE has been shown to have non-cell autonomous effects on lamination of the retina (Jensen et al., 2001; Jensen and Westerfield, 2004).

In addition to positioning defects, melanosome morphology was also disrupted in Shroom2-SPL-MO morphants (Fig. 6C,F). We were curious about the nature of these defects and so melanosome structure was further imaged with high magnification TEM (Fig. 7). A representative control RPE region is shown in Fig. 7A, in which melanosomes of various sizes are present, most of which show the dense black pigment accumulation and smooth-edged morphology typical of RPE melanosomes. By contrast, two representative regions of Shroom2-SPL-MO morphant RPE are shown in Fig. 7B. Overall melanosome number in Shroom2-SPL-MO morphants is similar to that in controls; however, the pigment density within these melanosome is in many instances decreased and their morphology is severely abnormal. Numerous small vesicular structures are obvious and in many cases these vesicles appear not to have coalesced into a single unit. This ‘bunch of grapes’ morphology may reflect a failure of endosomes to fuse as the melanosome develops.

In Shroom2-SPL-MO morphants, melanosome aggregates were nearly 90% larger in area than their control counterparts (Fig. 7C, $P<0.001$), again consistent with a defect in melanosome maturation (Cortese et al., 2005). We found the ‘bunch of grapes’ morphology to be intriguing, and we sought to quantify this defect with morphometric software. We analyzed melanosome shape using a ‘roundness’ function, which compares the predicted circumference based on radius to the actual circumference of an object. This function therefore quantifies the regularity of the surface of an object. A score of 1.00 indicates a perfect circle. We found that melanosomes in wild-type animals had a mean roundness of 1.36, owing to their normally elongate shape (Fig. 7A,D). By contrast, melanosomes in Shroom2-SPL-MO morphants had an average roundness of over 1.7, consistent with their highly irregular surfaces (Fig. 7B,D). This difference was statistically significant ($P<0.001$). Combined, these results indicate that Shroom2 is not only necessary for RPE pigmentation and the apical localization of RPE melanosomes, but also for melanosome biogenesis.

Rab27a is required for Shroom2-dependent melanosome distribution

We next sought to probe the mechanisms by which Shroom2 may function to govern RPE pigmentation. Using ectopic expression in naïve *Xenopus* blastomeres (see Fig. 2F), we have previously demonstrated that Shroom3-mediated pigment accumulation and apical constriction require the activity of the Rap1 GTPase (Haigo et al., 2003) (P.D.F., unpublished). We therefore tested for an interaction between Shroom2 and Rap1. Expression of high doses of dominant-negative Rap1-N17 mutant (Kitayama et al., 1990) had no effect on the ability of Shroom2 to elicit pigment accumulation in naïve blastomeres (Fig. 2E). Expression of high doses of Rap1GAP (Rubinfeld et al., 1991), which also inhibits Rap1 activity, likewise failed to inhibit Shroom2 activity when co-expressed in *Xenopus* blastomeres (Fig. 2E).

We next tested for interaction between Shroom2 and Rab27. This small GTPase is a crucial mediator of actin-mediated melanosome movement in the eye (Futter et al., 2004; Gibbs et al., 2004). *Rab27a*-null (*Ashen*) mice have melanosome distribution defects in the RPE, where the melanosomes cannot move beyond the adherens

junction to the apical processes (Futter et al., 2004). Given the hypopigmentation and melanosome distribution defects in Shroom2-SPL-MO morphants, Rab27a is a good candidate for mediating Shroom2 activity. For these experiments, we used dominant-negative mutations of Rab27a identified in humans with Griscelli syndrome, a disease characterized in part by albinism (Bahadoran et al., 2003; Menasche et al., 2003). The Rab27a-L130P missense mutation is unable to connect melanosomes to myosin and the actin cytoskeleton (Bahadoran et al., 2003), and both Rab27a-L130P and Rab27a-A152P mutations significantly interfere with the GTP and GDP binding activity of Rab27a (Menasche et al., 2003). Indeed, co-expression of either dominant-negative Rab27a-L130P or Rab27a-A152P inhibited the ability of Shroom2 to trigger pigment concentration in naïve cells (Fig. 2F). These observations place Rab27a downstream of Shroom2 in the control of melanosome distribution in epithelial cells and, furthermore, suggest that Shroom family members use distinct downstream effector GTPases in regulating cellular processes.

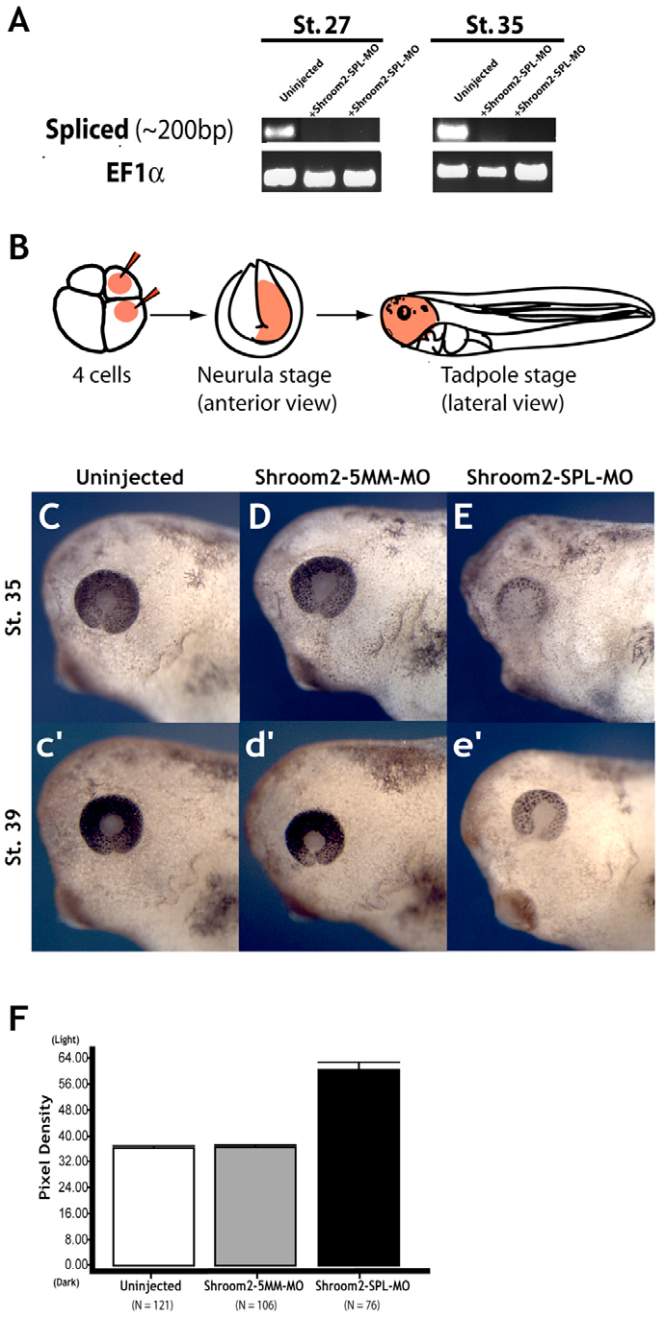

Fig. 5. Morpholino knock-down of Shroom2 results in severe RPE hypopigmentation. (**A**) RT-PCR confirmation of morpholino efficacy. Normally spliced Shroom2 mRNA was absent from 80 ng Shroom2-SPL-MO injected embryos. (**B**) Shroom2-SPL-MO or Shroom2-5MM-MO (80 ng) was injected into two animal blastomeres at the four-cell stage and embryos were grown to stage 42. (**C**,**D**) Shroom2-SPL-MO injected embryos show severe reduced RPE pigmentation (**E**,e′) when compared with stage-matched uninjected or Shroom-5MM-MO embryos (C-d′). (**F**) Measurement of pixel density in the eye indicates no significant difference in pigmentation between uninjected and Shroom2-5MM-MO-injected embryos at stage 39, but a drastic difference between pixel density between controls and Shroom2-SPL-MO eyes.

Shroom2 promotes apical accumulation of γ-tubulin in naïve epithelial cells

Melanosomes translocate apically first on microtubules and then along actin filaments (Maniak, 2003). Rab27 is thought to act at the level of the actin cytoskeleton, linking melanosomes to myosin motors that allow them to move along the apical actin network and into their final positions below the apical surface (Futter et al., 2004; Gibbs et al., 2004; Seabra and Coudrier, 2004). Our findings that Shroom2 expression does not elicit significant actin accumulation (Fig. 1I) and that it acts upstream of Rab27 (Fig. 2F) suggest a potential role for Shroom2 at the level of microtubules. This notion was intriguing in light of our recent finding that Shroom3, a protein

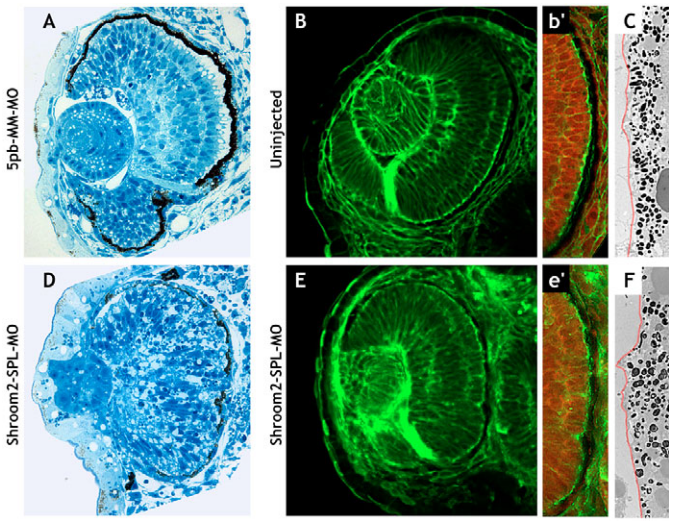

Fig. 6. Retinal lamination and RPE structure are disrupted in Shroom2-SPL-MO morphants. (**A**,**D**) Histological analysis indicated that the most severely affected Shroom2-SPL-MO morphants had prominent retinal lamination defects and increased numbers of pyknotic nuclei in their retinas when compared with stage-matched 5 bp-MM MO-injected controls. (**B**,**E**) Less severely affected morphants showed significantly better retinal lamination, as demonstrated here via actin localization in optical sections. Additionally, phalloidin staining revealed the regular appearance of the RPE in control embryos (B,b′) in contrast to that in Shroom2-SPL-MO morphants (E,e′) in which the RPE invaded the retina with numerous apical protrusions. (**C**,**F**) Further examination with TEM highlights these apical protrusions and also indicates that melanosome morphology and distribution are disrupted in Shroom2-SPL-MO morphants. Melanosomes appear clumpy and are not limited to the apical cell surface. Red lines delimit apical (left) and basal (right) surfaces of the RPE.

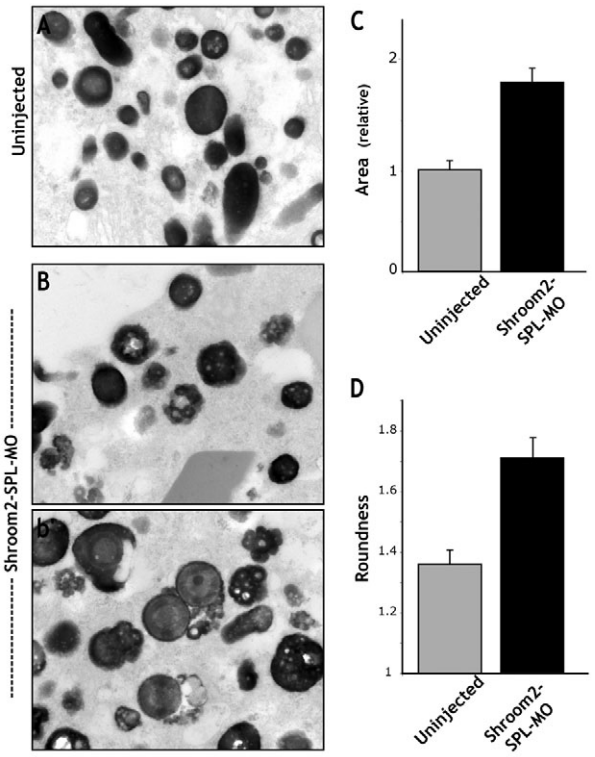

Fig. 7. Ultrastructural analysis of Shroom2 RPE. (**A**,**B**) High magnification TEM allowed further analysis of Shroom2-SPL-MO morphant melanosome morphology. (A) Control RPE contained smooth-edged melanosomes of varying size and black because of melanin accumulation. (B,b′) Two representative regions of Shroom2-SPL-MO morphant RPE. Melanosome number was similar to controls; however, melanosome morphology was severely abnormal. Melanosomes contained numerous vesicular structures, most of which appeared to have not coalesced into a single structure resulting in a 'bunch of grapes' morphology. (**C**) Measurement of relative melanosome area of melanosomes in Shroom2-SPL-MO morphants and controls, indicated that the melanosome aggregates of Shroom2 morphants were almost 90% larger in area than controls. (**D**) Shroom2-SPL-MO morphant melanosomes were also found to have highly irregular surfaces, with a relative roundness value of over 1.7 and compared with a value of 1.36 for control melanosomes (a perfect circle has a roundness of 1.00).

closely related to Shroom2, coordinates microtubule assembly in epithelial cells by governing the localization of the microtubule-nucleating component γ-tubulin (C. J. Lee, H. M. Scherr and J.B.W., unpublished).

We therefore asked if Shroom2 might share with Shroom3 the ability to govern γ-tubulin localization. Again, using naïve blastomeres (Fig. 1B), we expressed either Shroom2 or Shroom3 by mRNA injection, and assessed γ-tubulin distribution by immunohistochemistry. We found that expression of either protein resulted in a dramatic accumulation of γ-tubulin at the apical cell surface (Fig. 8A-C,a′-c′). Despite the differences in apical constriction and actin accumulation (Fig. 1F-I), Shroom2 and Shroom3 were equally effective in driving the re-localization of γ-tubulin. The accumulated γ-tubulin overlapped entirely with regions of pigment accumulation (Fig. 8A-C,a′-c′).

Our Shroom2 construct is myc-tagged and immunohistochemistry revealed that the effect of Shroom2 on γ-tubulin was cell-autonomous (Fig. 8D-F). Moreover, we found that Shroom2 protein, when expressed in naïve blastomeres, did not co-localize with the accumulated γ-tubulin. Rather, the Shroom2 signal decorated the cell surface immediately apical to the accumulated γ-tubulin (Fig. 8D-F).

DISCUSSION

In this paper, we provide the first developmental characterization of Shroom2, a member of the Shroom family of proteins. We show that expression of ectopic Shroom2 is sufficient to drive accumulation of pigment in epithelial cells, but that Shroom2, unlike Shroom3, does not elicit robust apical actin accumulation or apical constriction (Fig. 1). Conversely, we show that loss of Shroom2 function, using either mosaic expression of dominant-negative Shroom2 or MO knock-down, perturbs normal pigmentation of the eye in vivo (Figs 4, 5). Significantly, that Shroom2 is expressed in the developing eye and expression in the eye is restricted to the RPE in stage 40 embryos (Fig. 3). We show that the failure of pigmentation is associated with defects in both the biogenesis and the apical localization of RPE melanosomes (Figs 6, 7). Furthermore, we demonstrate epistatically that Shroom2 functions upstream of the Rab27 GTPase in regulating melanosome distribution and also that Shroom2 elicits γ-tubulin accumulation at the apical epithelial cell surface (Figs 2, 8). When combined, these results position Shroom2 at the interface of the actin- and microtubule-based cytoskeletons, and strongly suggest that the regulation of both of these is required for proper melanosome development and localization in the RPE.

Shroom2, RPE pigmentation and eye development

Melanosome biogenesis is a complex process that has only recently begun to be elucidated in vivo. Melanosomes derive from the endosomal network of the cell and go through several distinct stages of maturation to form the mature melanin-containing organelle (reviewed by Raposo and Marks, 2002). Shroom2 morphants show obvious RPE defects where melanosomes are larger than normal and appear to be composed of small vesicular bodies that have not coalesced into a uniform melanosome (Fig. 6). It is not clear at what step of the maturation process melanosome biogenesis is disrupted in these morphants, but our analysis of Shroom2 function makes it possible to propose an explanation.

We find that Shroom2 acts upstream of Rab27a and that Shroom2 is sufficient to drive apical accumulation of γ-tubulin, a crucial component of microtubule-nucleating complexes (Gunawardane et al., 2000; Job et al., 2003; Stearns et al., 1991). Given the known functions of γ-tubulin and its apical localization in RPE cells (Rizzolo and Joshi, 1993), we suggest that the principle role for Shroom2 is to regulate microtubule assembly in the RPE by governing the localization of γ-tubulin. Such a function for Shroom2 is consistent with the observed melanosome phenotype, as an intact microtubule cytoskeleton is known to be necessary for proper maturation and fusion of endosomes in epithelial cells (Bomsel et al., 1990; Clarke et al., 2002; Gruenberg et al., 1989). In addition to morphological defects, melanosomes in Shroom2 morphants also fail to localize properly to the apical surface of the RPE (Fig. 5). It is thought that apical deployment of melanosomes first involves movement on the microtubule cytoskeleton and then transfer to the actin cytoskeleton for final deployment (Maniak, 2003). As such, a role for Shroom2 in microtubule organization could also explain the failure of melanosomes to accumulate apically in morphants.

Loss of Shroom2 function also results in defects in retinal lamination and in anterior eye development (Fig. 5). We can envision several possible scenarios to account for the observed lamination

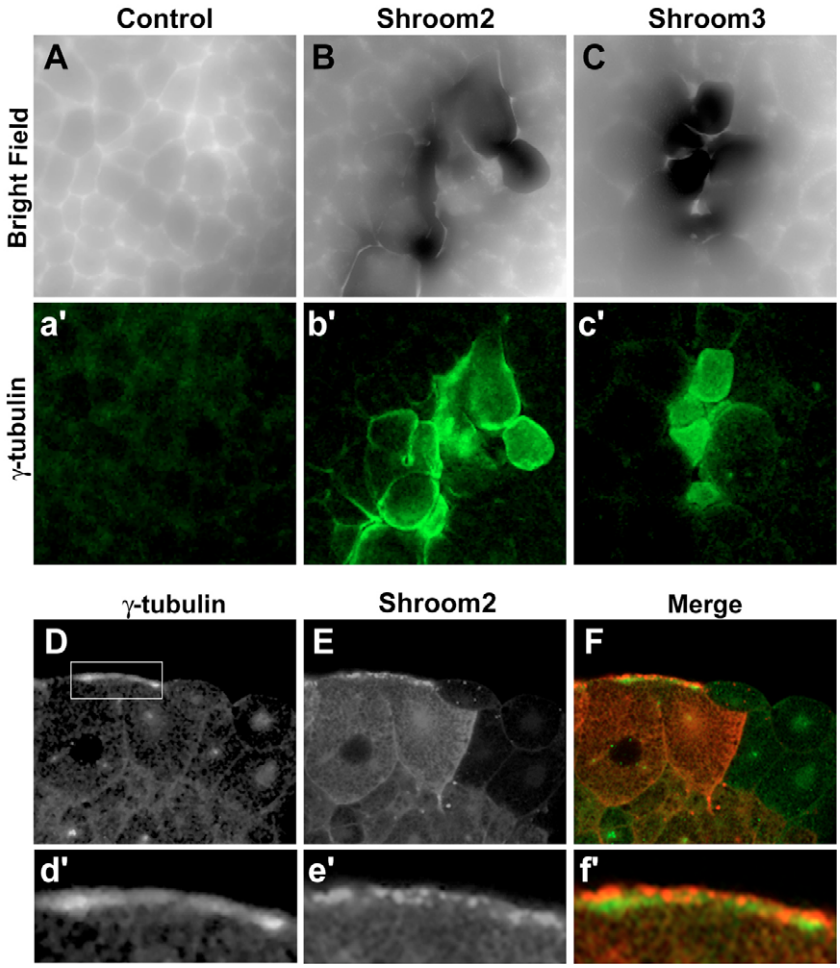

Fig. 8. Shroom2 expression induces the apical accumulation of γ-tubulin in epithelial cells. (**A-c'**) Both Shroom2 and Shroom3 expression in naïve blastomeres was found to trigger dramatic γ-tubulin accumulation at the apical cell surface of epithelial cells. (B-c′) γ-Tubulin accumulation overlapped entirely with regions of pigment accumulation and had the same intensity in both Shroom2 and Shroom3-expressing embryos (1 ng injected for either mRNA). (**D-f'**) Shroom2 expression (red) in naïve blastomeres did not co-localize with accumulated γ-tubulin (green), however, but localized at the cell surface basal to γ-tubulin.

defects. Shroom2 could play a direct role in the retina by regulating the survival of retinal cells, by influencing cell fate specification events during the early phases of retinal development or by dictating the final laminar position of differentiating retinal neurons. Shroom2 is expressed in the retinal neuroepithelium prior to neurogenesis (Fig. 3), making each of these scenarios formally possible. Alternatively, the observed lamination defects in Shroom2 morphants could be an indirect consequence of loss of Shroom2 function in the RPE. The RPE plays an important role in regulating retinal lamination (e.g. Raymond and Jackson, 1995). In fact, disruption of normal cell polarity specifically in the RPE is sufficient to induce lamination defects in the zebrafish retina (Jensen et al., 2001; Jensen and Westerfield, 2004). These defects could reflect a role for the Shroom2 protein in regulating the polarity of RPE cells. Finally, ocular albinos display macular hypoplasias where retinal morphogenesis is impaired in areas of the retina that are apposed to hypopigmented RPE (Jeffery, 1997), so our observed neural retina defects could be a result of observed defects in melanosome biogenesis in the RPE. Further studies will be required to elucidate the molecular basis for the lamination defects and the anterior segment defects in Shroom2 morphants and to determine if they result from direct roles of Shroom2 in this process.

Shroom2 and the Shroom family of proteins

Our data are most consistent with the view that Shroom2 functions at the level of microtubules. In addition, such a role for Shroom2 is supported by our recent finding that Shroom3, a closely related protein, also governs γ-tubulin localization and microtubule assembly (C. J. Lee, H. M. Scherr and J.B.W., unpublished). These data may suggest that microtubule organization is a key function of Shroom family proteins in general. However, we show here that γ-tubulin and Shroom2 do not co-localize apically (Fig. 8D-F). It is relevant then to point out that while Shroom2 has minimal effect on actin when overexpressed (Fig. 1I), the other family members, Shroom1, Shroom3 and Shroom4, are each associated with the actin cytoskeleton (Dietz et al., 2006; Hagens et al., 2005; Haigo et al., 2003; Hildebrand, 2005; Zuckerman et al., 1999). As such, it is possible be that Shroom2 itself is localized apically by association with actin, and in turn drives the apical localization of γ-tubulin. One intriguing possibility is that a general function for Shroom family proteins is to link the actin and microtubule cytoskeletons.

Shroom2 and ocular albinism in humans

RPE pigmentation deficiencies in humans with Type I X-linked ocular albinism result in a loss of visual acuity stemming from defective melanosome biogenesis and hypopigmentation of the RPE (Shen et al., 2001). Mutations in the OA1 gene are thought to underlie X-linked ocular albinism, but mutations in this gene have not been identified in all individuals (Bassi et al., 1995; Schiaffino et al., 1995a; Tijmes et al., 1998). Furthermore, a second distinct human pigmentation disorder for which no causative mutations have been identified, ocular albinism with sensorineural deafness (OASD), also maps to the same region of the X-chromosome (Tak et al., 2004; Winship et al., 1993). The locus encoding human

Shroom2 lies within the crucial region for these albinism-associated disorders, and the Shroom2 gene is immediately adjacent to OA1 on the human X-chromosome (Schiaffino et al., 1995b), as it is in *Xenopus tropicalis* (not shown). We have demonstrated herein that Shroom2 loss of function results in striking RPE pathologies that include hypopigmentation stemming from melanosome biogenesis and localization defects, similar to those observed in individuals with ocular albinism and mouse models (e.g. Cortese et al., 2005; Tak et al., 2004). That the locus encoding human Shroom2 lies within the genomic region associated with two distinct forms of ocular albinism suggests that Shroom2 mutations may possibly be a contributing factor in these human visual system disorders. These data suggest that further studies are needed in humans with ocular albinism, and that a detailed analysis of the Shroom2 locus should be undertaken in individuals with OASD or ocular albinism type I in which OA1 mutations are not present.

We thank Richard Harland for critical insights into this project; John Sisson, Vittoria Schiaffino, Andrea Ballabio, Arturo DeLozanne and Terry O'Halloran for helpful discussions; and Louise Trakimas and John Mendenhall for TEM assistance. We thank the Kirschner laboratory for the gift of *Xenopus* γ-tubulin antibody. This work was supported by grants from the Knights Templar Eye Foundation and American Health Assistance Foundation Macular Degeneration Research Program (#M2006-024) to J.M.G.; by a grant from NIH (1RO1GM74104) to J.B.W.; and by a Career Award in the Biomedical Sciences from the Burroughs Wellcome Fund to J.B.W.

References

Apodaca, G. (2001). Endocytic traffic in polarized epithelial cells: role of the actin and microtubule cytoskeleton. *Traffic* **2**, 149-159.

Back, I., Donner, K. O. and Reuter, T. (1965). The screening effect of the pigment epithelium on the retinal rods in the frog. *Vision Res.* **5**, 101-111.

Bahadoran, P., Busca, R., Chiaverini, C., Westbroek, W., Lambert, J., Bille, K., Valony, G., Fukuda, M., Naeyaert, J. M., Ortonne, J. P. et al. (2003). Characterization of the molecular defects in Rab27a, caused by RAB27A missense mutations found in patients with Griscelli syndrome. *J. Biol. Chem.* **278**, 11386-11392.

Barral, D. C. and Seabra, M. C. (2004). The melanosome as a model to study organelle motility in mammals. *Pigment Cell Res.* **17**, 111-118.

Bassi, M. T., Schiaffino, M. V., Renieri, A., De Nigris, F., Galli, L., Bruttini, M., Gebbia, M., Bergen, A. A., Lewis, R. A. and Ballabio, A. (1995). Cloning of the gene for ocular albinism type 1 from the distal short arm of the X chromosome. *Nat. Genet.* **10**, 13-19.

Bomsel, M., Parton, R., Kuznetsov, S. A., Schroer, T. A. and Gruenberg, J. (1990). Microtubule- and motor-dependent fusion in vitro between apical and basolateral endocytic vesicles from MDCK cells. *Cell* **62**, 719-731.

Burnside, B., Adler, R. and O'Connor, P. (1983). Retinomotor pigment migration in the teleost retinal pigment epithelium. I. Roles for actin and microtubules in pigment granule transport and cone movement. *Invest. Ophthalmol. Vis. Sci.* **24**, 1-15.

Chalmers, A. D., Strauss, B. and Papalopulu, N. (2003). Oriented cell divisions asymmetrically segregate aPKC and generate cell fate diversity in the early Xenopus embryo. *Development* **130**, 2657-2668.

Chalmers, A. D., Pambos, M., Mason, J., Lang, S., Wylie, C. and Papalopulu, N. (2005). aPKC, Crumbs3 and Lgl2 control apicobasal polarity in early vertebrate development. *Development* **132**, 977-986.

Clarke, M., Kohler, J., Heuser, J. and Gerisch, G. (2002). Endosome fusion and microtubule-based dynamics in the early endocytic pathway of dictyostelium. *Traffic* **3**, 791-800.

Cortese, K., Giordano, F., Surace, E. M., Venturi, C., Ballabio, A., Tacchetti, C. and Marigo, V. (2005). The Ocular Albinism Type 1 (OA1) gene controls melanosome maturation and size. *Invest. Ophthalmol. Vis. Sci.* **46**, 4358-4364.

Dietz, M. L., Bernaciak, T. M., Vendetti, F. and Hildebrand, J. D. (2006). Differential actin-dependent localization modultes the evolutionarily conserved activity of shroom-family proteins. *J. Biol. Chem.* **281**, 20542-20554.

Dollar, G. L., Weber, U., Mlodzik, M. and Sokol, S. Y. (2005). Regulation of Lethal giant larvae by Dishevelled. *Nature* **437**, 1376-1380.

Futter, C. E., Ramalho, J. S., Jaissle, G. B., Seeliger, M. W. and Seabra, M. C. (2004). The role of Rab27a in the regulation of melanosome distribution within retinal pigment epithelial cells. *Mol. Biol. Cell* **15**, 2264-2275.

Gibbs, D., Azarian, S. M., Lillo, C., Kitamoto, J., Klomp, A. E., Steel, K. P., Libby, R. T. and Williams, D. S. (2004). Role of myosin VIIa and Rab27a in the motility and localization of RPE melanosomes. *J. Cell Sci.* **117**, 6473-6483.

Gruenberg, J., Griffiths, G. and Howell, K. E. (1989). Characterization of the early endosome and putative endocytic carrier vesicles in vivo and with an assay of vesicle fusion in vitro. *J. Cell Biol.* **108**, 1301-1316.

Gunawardane, R. N., Lizarraga, S. B., Wiese, C., Wilde, A. and Zheng, Y. (2000). gamma-Tubulin complexes and their role in microtubule nucleation. *Curr. Top. Dev. Biol.* **49**, 55-73.

Hagens, O., Dubos, A., Abidi, F., Barbi, G., Van Zutven, L., Hoeltzenbein, M., Tommerup, N., Moraine, C., Fryns, J. P., Chelly, J. et al. (2005). Disruptions of the novel KIAA1202 gene are associated with X-linked mental retardation. *Hum. Genet.* **118**, 578-590.

Hagens, O., Ballabio, A., Kalscheuer, V., Kraehenbuhl, J. P., Schiaffino, M. V., Smith, P. R., Staub, O., Hildebrand, J. and Wallingford, J. B. (2006). A new standard nomenclature for proteins related to Apx and Shroom. *BMC Cell Biol.* **7**, 18.

Haigo, S. L., Hildebrand, J. D., Harland, R. M. and Wallingford, J. B. (2003). Shroom induces apical constriction and is required for hingepoint formation during neural tube closure. *Curr. Biol.* **13**, 2125-2137.

Hildebrand, J. D. (2005). Shroom regulates epithelial cell shape via the apical positioning of an actomyosin network. *J. Cell Sci.* **118**, 5191-5203.

Hildebrand, J. D. and Soriano, P. (1999). Shroom, a PDZ domain-containing actin-binding protein, is required for neural tube morphogenesis in mice. *Cell* **99**, 485-497.

Jeffery, G. (1997). The albino retina: an abnormality that provides insight into normal retinal development. *Trends Neurosci.* **20**, 165-169.

Jensen, A. M. and Westerfield, M. (2004). Zebrafish mosaic eyes is a novel FERM protein required for retinal lamination and retinal pigmented epithelial tight junction formation. *Curr. Biol.* **14**, 711-717.

Jensen, A. M., Walker, C. and Westerfield, M. (2001). mosaic eyes: a zebrafish gene required in pigmented epithelium for apical localization of retinal cell division and lamination. *Development* **128**, 95-105.

Job, D., Valiron, O. and Oakley, B. (2003). Microtubule nucleation. *Curr. Opin. Cell Biol.* **15**, 111-117.

King-Smith, C., Paz, P., Lee, C. W., Lam, W. and Burnside, B. (1997). Bidirectional pigment granule migration in isolated retinal pigment epithelial cells requires actin but not microtubules. *Cell Motil. Cytoskeleton* **38**, 229-249.

Kitayama, H., Matsuzaki, T., Ikawa, Y. and Noda, M. (1990). Genetic analysis of the Kirsten-ras-revertant 1 gene: potentiation of its tumor suppressor activity by specific point mutations. *Proc. Natl. Acad. Sci. USA* **87**, 4284-4288.

Maniak, M. (2003). Organelle transport: a park-and-ride system for melanosomes. *Curr. Biol.* **13**, R917-R919.

Marks, M. S. and Seabra, M. C. (2001). The melanosome: membrane dynamics in black and white. *Nat. Rev. Mol. Cell Biol.* **2**, 738-748.

McNeil, E. L., Tacelosky, D., Basciano, P., Biallas, B., Williams, R., Damiani, P., Deacon, S., Fox, C., Stewart, B., Petruzzi, N. et al. (2004). Actin-dependent motility of melanosomes from fish retinal pigment epithelial (RPE) cells investigated using in vitro motility assays. *Cell Motil. Cytoskeleton* **58**, 71-82.

Menasche, G., Feldmann, J., Houdusse, A., Desaymard, C., Fischer, A., Goud, B. and de Saint Basile, G. (2003). Biochemical and functional characterization of Rab27a mutations occurring in Griscelli syndrome patients. *Blood* **101**, 2736-2742.

Newport, J. and Kirschner, M. (1982). A major developmental transition in early Xenopus embryos: II. Control of the onset of transcription. *Cell* **30**, 687-696.

Nieuwkoop, P. D. and Faber, J. (1994). *Normal Table of Xenopus laevis (Daudin).* New York: Garland.

Ohnuma, S., Mann, F., Boy, S., Perron, M. and Harris, W. A. (2002). Lipofection strategy for the study of Xenopus retinal development. *Methods* **28**, 411-419.

Prat, A. G., Holtzman, E. J., Brown, D., Cunningham, C. C., Reisin, I. L., Kleyman, T. R., McLaughlin, M., Jackson, G. R., Jr, Lydon, J. and Cantiello, H. F. (1996). Renal epithelial protein (Apx) is an actin cytoskeleton-regulated Na+ channel. *J. Biol. Chem.* **271**, 18045-18053.

Raposo, G. and Marks, M. S. (2002). The dark side of lysosome-related organelles: specialization of the endocytic pathway for melanosome biogenesis. *Traffic* **3**, 237-248.

Raymond, S. M. and Jackson, I. J. (1995). The retinal pigmented epithelium is required for development and maintenance of the mouse neural retina. *Curr. Biol.* **5**, 1286-1295.

Rizzolo, L. J. and Joshi, H. C. (1993). Apical orientation of the microtubule organizing center and associated gamma-tubulin during the polarization of the retinal pigment epithelium in vivo. *Dev. Biol.* **157**, 147-156.

Roberts, S. J., Leaf, D. S., Moore, H. P. and Gerhart, J. C. (1992). The establishment of polarized membrane traffic in Xenopus laevis embryos. *J. Cell Biol.* **118**, 1359-1369.

Rubinfeld, B., Munemitsu, S., Clark, R., Conroy, L., Watt, K., Crosier, W. J., McCormick, F. and Polakis, P. (1991). Molecular cloning of a GTPase activating protein specific for the Krev-1 protein p21rap1. *Cell* **65**, 1033-1042.

Schiaffino, M. V., Bassi, M. T., Galli, L., Renieri, A., Bruttini, M., De Nigris, F., Bergen, A. A., Charles, S. J., Yates, J. R., Meindl, A. et al. (1995a). Analysis of the OA1 gene reveals mutations in only one-third of patients with X-linked ocular albinism. *Hum. Mol. Genet.* **4**, 2319-2325.

Schiaffino, M. V., Bassi, M. T., Rugarli, E. I., Renieri, A., Galli, L. and Ballabio, A. (1995b). Cloning of a human homologue of the Xenopus laevis APX gene from the ocular albinism type 1 critical region. *Hum. Mol. Genet.* **4**, 373-382.
Seabra, M. C. and Coudrier, E. (2004). Rab GTPases and myosin motors in organelle motility. *Traffic* **5**, 393-399.
Shen, B., Samaraweera, P., Rosenberg, B. and Orlow, S. J. (2001). Ocular albinism type 1, more than meets the eye. *Pigment Cell Res.* **14**, 243-248.
Sive, H. L., Grainger, R. M. and Harland, R. M. (2000). *Early Development of Xenopus laevis: A Laboratory Manual.* Cold Spring Harbor: Cold Spring Harbor Laboratory Press.
Staub, O., Verrey, F., Kleyman, T. R., Benos, D. J., Rossier, B. C. and Kraehenbuhl, J. P. (1992). Primary structure of an apical protein from Xenopus laevis that participates in amiloride-sensitive sodium channel activity. *J. Cell Biol.* **119**, 1497-1506.
Stearns, T., Evans, L. and Kirschner, M. (1991). Gamma-tubulin is a highly conserved component of the centrosome. *Cell* **65**, 825-836.
Tak, W. J., Kim, M. N., Hong, C. K., Ro, B. I., Song, K. Y. and Seo, S. J. (2004). Ocular albinism with sensorineural deafness. *Int. J. Dermatol.* **43**, 290-292.
Tijmes, N. T., Bergen, A. B. and De Jong, P. T. (1998). Paucity of signs in X linked ocular albinism with a 700 kb deletion spanning the OA1 gene. *Br. J. Ophthalmol.* **82**, 457-458.
Troutt, L. L. and Burnside, B. (1989). Role of microtubules in pigment granule migration in teleost retinal pigment epithelial cells. *Exp. Eye Res.* **48**, 433-443.
Winship, I. M., Babaya, M. and Ramesar, R. S. (1993). X-linked ocular albinism and sensorineural deafness: linkage to Xp22.3. *Genomics* **18**, 444-445.
Zuckerman, J. B., Chen, X., Jacobs, J. D., Hu, B., Kleyman, T. R. and Smith, P. R. (1999). Association of the epithelial sodium channel with Apx and alpha-spectrin in A6 renal epithelial cells. *J. Biol. Chem.* **274**, 23286-23295.